

Available online at www.sciencedirect.com

SciVerse ScienceDirect

Energy Procedia 22 (2012) 61 – 66

Energy
Procedia

E-MRS 2011 Spring Meeting Symposium T

Perovskite-type LaTiO₂N oxynitrides for solar water splitting: Influence of the synthesis conditions

Alexandra E. Maegli^a, Eugenio H. Otal^a, Takashi Hisatomi^b, Songhak Yoon^a, Céline M. Leroy^b, Nina Schäuble^a, Ye Lu^a, Michael Grätzel^b, Anke Weidenkaff^{a*}

^aLaboratory for Solid State Chemistry and Catalysis, Empa - Swiss Federal Laboratories for Materials Science and Technology, 8600 Dübendorf, Switzerland

^bLaboratory of Photonics and Interfaces, EPFL - Swiss Federale Institute of Technology Lausanne, 1015 Lausanne, Switzerland

Abstract

Oxynitrides with the nominal composition LaTiO₂N were prepared from a La₂Ti₂O₇ precursor by thermal ammonolysis of the oxide under an NH₃ flow for different durations t (4 – 30 h). X-ray diffraction (XRD) indicated that phase-pure LaTiO₂N samples were obtained when $t \geq 13$ h. The material was further characterised by scanning electron microscopy (SEM), surface area measurements based on the BET method, thermogravimetric analysis (TGA) and UV-visible diffuse reflectance spectroscopy (DRS). The powders displayed an increased crystallite size and a decreased surface area with increasing t . The ratio of N/(N+O) increased with t from 0.22 – 0.27. Correlated to this nitrogen increase, a small variation of the bandgap energy was observed from 2.19 to 2.12 eV with t . All LaTiO₂N samples oxidised H₂O into O₂ in the presence of an electron acceptor (Ag⁺). The O₂ evolution was increased from 12 μmol/h ($t = 13$ h) to 22 – 24 μmol/h ($16 \text{ h} \leq t \leq 30 \text{ h}$). It was found that the nitrogen content and the amount of defects played a key role in the photocatalytic O₂ evolution.

© 2012 Published by Elsevier Ltd. Selection and/or peer review under responsibility of European Material Research Society (E-MRS)
Open access under [CC BY-NC-ND license](https://creativecommons.org/licenses/by-nc-nd/4.0/).

Keywords: LaTiO₂N; Oxynitride; Photocatalysis; Ammonolysis; Perovskite

1. Introduction

Oxynitrides are an emerging class of materials which are interesting for photocatalytic applications because their bandgap is in the range of visible light potentially allowing them to harvest sunlight more efficiently [1]. Besides an appropriate band structure, other criteria like a large surface area, good crystallinity and a small defect concentration have to be met to enable the compound to show a good photocatalytic performance [2].

Perovskite-type materials are known for various kinds of applications because their crystal structure is very flexible towards substitutions which may induce interesting physical properties such as colossal magnetoresistance [3], superconductivity [4], *etc.* Most substitutions concern the A- and B-site of the perovskite lattice, but substitution

of the oxygen sites with *e.g.* nitrogen offers a powerful way to alter the electronic structure of the valence band [5-7]. The valence band of the perovskite-type oxides is formed of deep lying oxygen orbitals (O 2*p*) resulting in a large bandgap [8]. Yet, when oxygen is partially substituted by nitrogen, the N 2*p* levels are located above the O 2*p* levels forcing the bandgap to decrease [9,10]. LaTiO₂N is an example of such a perovskite-type oxynitride and its structure [11,12] and photocatalytic activity [13,14] have been previously investigated.

The scope of the presented work was to investigate the influence of the ammonolysis duration *t* upon the physico-chemical properties, *e.g.* the crystallite size, surface area and nitrogen content, and subsequently the O₂ evolution activity of the material. We intended to prove that a fine-tuning of the preparation conditions could influence the photocatalytic activity of LaTiO₂N substantially and allow for enhanced performance.

2. Experimental

The La₂Ti₂O₇ oxide powder was synthesised by a soft-chemistry method with citric acid (CA) and ethylene glycol (EG) as complexing agents. The molar ratio of the cations (lanthanum and titanium), EG and CA was at the ratio of La/Ti/EG/CA = 1/1/40/10. Ti(OCH(CH₃)₂)₄ (Sigma-Aldrich, ≥ 99.999 %) was added to EG (Merck, ≥ 99.5 %), therein CA (Alfa Aesar, ≥ 99 %) and La(NO₃)₃·6(H₂O) (Merck, > 99.0 %) was appended. This mixture was stirred under reflux at T = 80 °C for 4 h and subsequently heated overnight at T = 120 °C to complete the complex formation and to promote the esterification between CA and EG. The obtained gel was slowly heated up to T = 200 °C and then calcined at T = 1000 °C for 6 h. The as-synthesised white oxide powder was treated under flowing NH₃ at elevated temperatures to transform it into LaTiO₂N oxynitrides (thermal ammonolysis). In detail, batches of 2 g of the oxide powder were inserted into an alumina cavity reactor which was flushed with NH₃ (Messer, ≥ 99.98 %) for 5 min before introducing the reactor into the furnace at T = 950 °C. The NH₃ flow during the synthesis was 200 mL/min and after the completed reaction, the samples were quenched to room temperature within a couple of minutes by removing the reactor from the furnace. Thereby, the ammonolysis time *t* was varied from 4 to 30 h.

XRD data were collected with a PANalytical X'Pert PRO θ-2θ scan system equipped with Johansson monochromator and an X'Celerator linear detector. The incident X-rays had a wavelength of 1.5406 Å (Cu-K_{α1}). The patterns were scanned from 20° to 80° (2θ). The crystallite size was determined by the Scherrer equation. The morphology of the samples was studied with scanning electron microscopy (SEM) using a Hitachi-S-4800 and a FEI Nova NanoSEM. The surface area was measured with a Micromeritics ASAP 2020 instrument by adsorption of N₂. UV-Visible diffuse reflectance spectra were collected with a UV-3600 Shimadzu UV-VIS-NIR spectrophotometer with an integrating sphere over a spectral range of 300 – 1200 nm (4.13 – 1.03 eV). The Kubelka-Munk function was applied to approximate the bandgap energy. The nitrogen content was determined by thermogravimetric analysis (TGA) with a NETZSCH STA 409 CD. Around 0.05 g of each oxynitride was heated in an Al₂O₃ crucible with 10 °C/min up to 1500 °C in a 50 mL/min flow of synthetic air. The nitrogen content was calculated from the total weight change after the thermal reoxidation of the oxynitride. The photocatalytic O₂ evolution test reaction was carried out with 0.1 g of the catalyst (LaTiO₂N) in a 10 mM AgNO₃ solution under irradiation of a 150 W halogen lamp. The pH of the solution was buffered to pH = 8 – 9 by adding 0.2 g La₂O₃ [15].

3. Results and Discussion

The XRD patterns illustrate the continuous transformation of the layered pyrochlore-type structure (La₂Ti₂O₇) into the perovskite-type structure (LaTiO₂N) with increasing ammonolysis time *t*. The structural transformation was completed after *t* = 13 h leading to phase-pure LaTiO₂N samples for *t* ≥ 13 h (Figure 1).

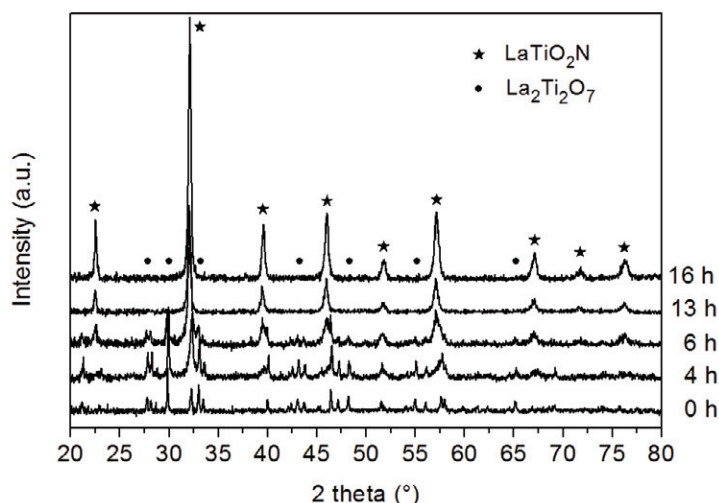


Fig. 1 XRD patterns showing the phase transformation from the layered perovskite-type oxide $\text{La}_2\text{Ti}_2\text{O}_7$ into the perovskite-type oxynitride LaTiO_2N . Phase-pure LaTiO_2N samples were achieved if $t \geq 13$ h. The dots and stars indicate the reflections of the $\text{La}_2\text{Ti}_2\text{O}_7$ and LaTiO_2N phase, respectively.

Figure 2 (a) and (b) show the morphology of the pristine oxide and the ammonolysed sample for $t = 16$ h, respectively. The oxide had a broad size distribution ranging from hundreds of nanometer to tens of micrometer and the larger chunks comprised smaller primary particles. The oxynitride sample had a more narrow size distribution and showed more uniform particle shapes compared to the oxide. The average particle size of the oxynitride sample was about 100 nm and the individual particles were connected to each other.

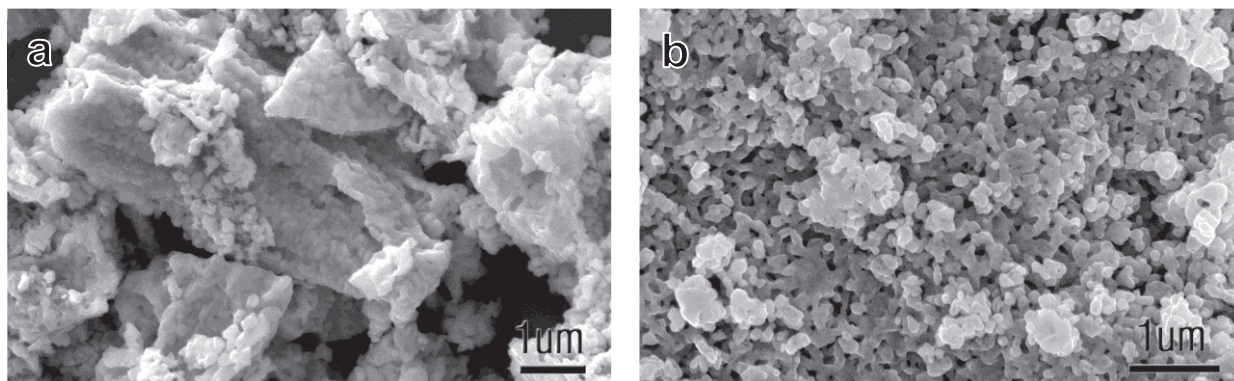


Fig. 2 SEM images of the (a) oxide sample $\text{La}_2\text{Ti}_2\text{O}_7$ and (b) oxynitride sample LaTiO_2N ammonolysed for $t = 16$ h.

All oxynitrides have distinctively smaller crystallite sizes (37 – 48 nm) than the pristine oxide (216 nm) (Table 1). This behaviour was in agreement with the surface area which was larger for all LaTiO_2N samples (17 – 9 m^2/g) compared to the $\text{La}_2\text{Ti}_2\text{O}_7$ powder (4 m^2/g). The extended ammonolysis reaction allowed crystallite growth and in turn reduced the surface area, yet these variations were relatively small. SEM images as well as the crystallite sizes and the surface areas illustrated that at the initial stage of the nitrogen insertion, the large oxide crystallites collapsed and smaller oxynitride crystallites could evolve.

Table 1 Crystallite size, surface area and bandgap energy of the pristine oxide and the phase-pure LaTiO₂N oxynitrides.

Phase	Ammonolysis time <i>t</i>	Crystallite size (nm)	Surface area (m ² /g)	Bandgap energy (eV)
La ₂ Ti ₂ O ₇	0	216	4	3.9
LaTiO ₂ N	13	37	17	2.19
	16	41	15	2.15
	20	42	14	2.15
	24	41	15	2.14
	30	48	9	2.12

Figure 3 indicates the continuous nitrogen uptake during the prolongation of the ammonolysis reaction. The measured ratio of N/(N+O) revealed that the nitrogen content was lower than the theoretical value (0.33) for the formula of LaTiO₂N. A similar nitrogen deficiency has been reported elsewhere [10,16]. This together with the information obtained from XRD allowed picturing the ammonolysis reaction as a continuous process. The reduction of the layered oxide into the perovskite-type oxynitride had no intermediate species; every step of the reaction showed a weighted mix of the initial and final phase with no presence of other phases. After 13 h of ammonolysis, a pure perovskite-type structure was obtained. It was found experimentally that a further nitridation under conservation of the perovskite structure was possible because O²⁻ ions were indeed substituted by N³⁻. The effects of the nitrogen non-stoichiometry and the increase of the nitrogen content with *t* on the subsequent charge-balance mechanisms (oxygen vacancies and/or Ti³⁺ interstitials) are not yet fully resolved.

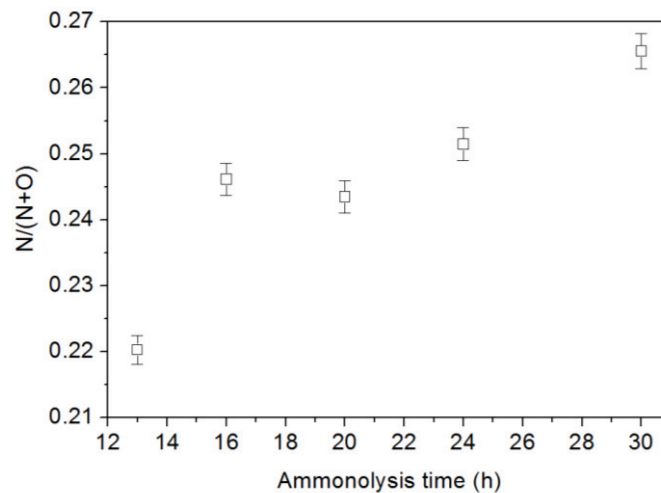


Fig. 3 Increasing nitrogen content with increasing ammonolysis time *t*. The ratio N/(N+O) was calculated from TGA.

The absorbance spectra of the oxynitrides shown in Figure 4 proved that the nitrogen substitution shifted the absorption edge wavelength to about 590 nm, giving the samples their distinctive reddish-brownish colour. Analysis of the absorption edge revealed that the bandgap energy of the oxynitrides decreased with *t* from 2.19 to 2.12 eV (Table 1). This is in agreement with the slightly increasing nitrogen content with *t* (Figure 3) and previously reported values [13,16,17] and should be suitable for the direct solar water splitting reaction with photoelectrochemical cells [18]. The absorbance after the absorption edge wavelength increased with the ammonolysis time *t*, which is in accordance with the literature [15]. It has been shown that this absorbance is correlated to the amount of defects mostly-associated with reduced Ti³⁺ species in the material [15,19].

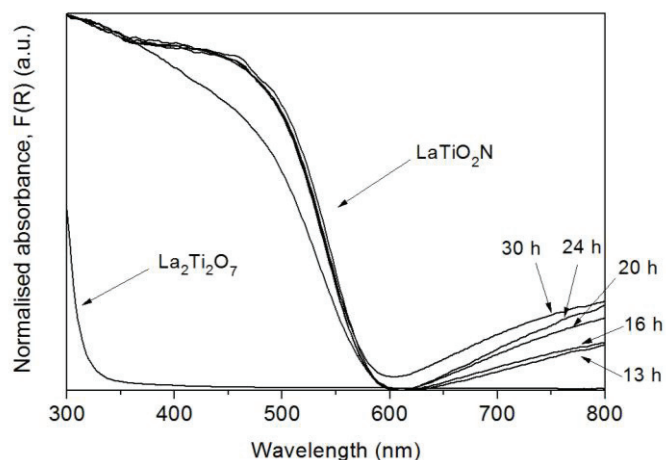


Fig. 4 Absorbance of the $\text{La}_2\text{Ti}_2\text{O}_7$ and the LaTiO_2N samples nitrided for different times.

Figure 5 shows the O_2 evolution activity for the different samples of LaTiO_2N . An increased activity from $12 \mu\text{mol/h}$ ($t = 13 \text{ h}$) to $22 - 24 \mu\text{mol/h}$ ($16 \text{ h} \leq t \leq 30 \text{ h}$) was observed. After reaching a value of around $22 \mu\text{mol/h}$, the prolongation of the ammonolysis reaction time did not further increase the O_2 evolution activity. Because the bandgap energy was found to be nearly constant, here, the O_2 evolution performance will be determined mainly by four variables: the nitrogen content, the surface area, the crystallinity and the amount of defects acting as recombination centres of the charge carriers. Whilst an increase of the first three factors is beneficial for the O_2 evolution, the last factor is counteracting. To discriminate the most important factor(s) for our samples, we will first compare the oxynitride ammonolysed for 13, 16 and 20 h. Table 1 clearly illustrates that the surface area and crystallinity varied on a very small scale between these three samples. Furthermore, the defect concentration in these samples was relatively low (Figure 4) and their negative influence on the photocatalytic performance would be tentatively negligible. Judging from the close correlation between the O_2 evolution rates and the $\text{N}/(\text{N}+\text{O})$ ratios for the first three samples, it would be reasonable to consider that the most important factor on the O_2 evolution was the nitrogen content in the early stage of the nitridation. The second group (sample $t = 24$ and 30 h) exhibited an O_2 evolution lower than the expectations which were based on their higher nitrogen contents compared to the previous samples. Assuming a trade-off between the increasing crystallite sizes and the decreasing surface areas with t , one possible explanation for the negligible enhancement of the activity for these two samples is that the defect concentration (*e.g.* reduced Ti^{3+} species) was increased. Recombination centres arising from such defects might have negated the beneficial increase of the nitrogen content.

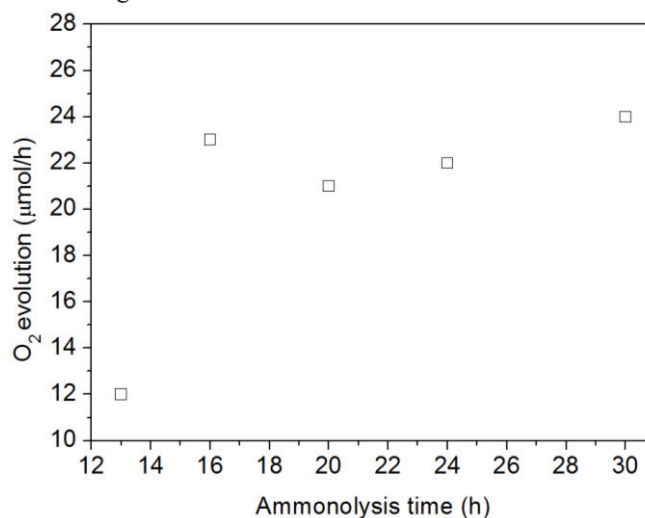


Fig. 5 O_2 evolution rate of 0.1 g LaTiO_2N in an aqueous solution containing 10 mM AgNO_3 .

4. Summary and Conclusion

Perovskite-type LaTiO_2N oxynitrides were prepared from oxide precursors ($\text{La}_2\text{Ti}_2\text{O}_7$) via thermal ammonolysis for different time durations t . Phase-pure LaTiO_2N samples were obtained by ammonolysis longer than 13 h. It was shown that the crystallite size increased with the thermal annealing during the ammonolysis ($t = 13 - 30$ h) and consequently the surface area decreased. The nitrogen content $\text{N}/(\text{N}+\text{O})$ increased with t from 0.22 – 0.27, yet, all samples showed nitrogen deficiency respective to the theoretical value (0.33). The bandgap energy was found to decrease with t from 2.19 to 2.12 eV because of the increase of nitrogen with t . All samples were photoactive, but with the prolongation of the ammonolysis time from 13 h to longer than 16 h, the O_2 evolution rate could be doubled (from 12 to 24 $\mu\text{mol}/\text{h}$). Therefore, it can be concluded that the preparation conditions of the powder had a substantial influence on the photocatalytic activity of LaTiO_2N . The investigation of several crucial influence parameters such as the crystallinity, the surface area, the nitrogen content and the amount of defects led to the conclusion that for shorter ammonolysis times ($t = 13, 16$ and 20 h), the amount of the nitrogen incorporation played a key role. Prolongation of the ammonolysis time ($t = 24$ and 30 h) indeed led to a further increase of the nitrogen content but it also evoked an increased defect formation having a negative influence on the photocatalytic O_2 evolution. The exact nature of these defects is a highly important and interesting issue which will be further investigated.

Acknowledgement

Financial support by the European Commission (Project NanoPEC, contract number 227179) is gratefully acknowledged.

References

- [1] K. Maeda and K. Domen, MRS Bulletin 36 (2011) 25.
- [2] A. Kudo and Y. Miseki, Chem. Soc. Rev. 38 (2009) 253.
- [3] M. Uehara, S. Mori, C.H. Chen, S.W. Cheong, Nature 399 (1999) 560.
- [4] T. He, Q. Huang, A.P. Ramirez, Y. Wang, K.A. Regan, N. Rogado, M.A. Hayward, M.K. Haas, J.S. Slusky, K. Inumara, et al., Nature 411 (2001) 54.
- [5] S.G. Ebbinghaus, H.-P. Abicht, R. Dronskowski, T. Müller, A. Reller, A. Weidenkaff, Prog. Solid State Chem. 37 (2009) 173.
- [6] M. Jansen and H.P. Lertschert, Nature 404 (2000) 980.
- [7] Y.-I. Kim and P.M. Woodward, J. Solid State Chem. 180 (2007) 3224.
- [8] H.W. Eng, P.W. Barnes, B.M. Auer, P.M. Woodward, J. Solid State Chem. 175 (2003) 91.
- [9] R. Aguiar, D. Logvinovich, A. Weidenkaff, A. Rachel, A. Reller, S.G. Ebbinghaus, Dyes Pigm 76 (2008) 70.
- [10] L. Le Paven-Thivet, L. Le Gendre, J. Le Castrec, F. Cheviré, F. Tessier, J. Pinel, Prog. Solid State Chem. 35 (2007) 299.
- [11] D. Logvinovich, L. Bocher, D. Sheptyakov, R. Figi, S.G. Ebbinghaus, R. Aguiar, M.H. Aguirre, A. Reller, Solid State Sci. 11 (2009) 1513.
- [12] M. Yashima, M. Saito, H. Nakano, T. Takata, K. Ogisu, K. Domen, Chem. Commun. 46 (2010) 4704.
- [13] A. Kasahara, K. Nukumizu, G. Hitoki, T. Takata, J.N. Kondo, M. Hara, H. Kobayashi, K. Domen, J. Phys. Chem. A 106 (2002) 6750.
- [14] R. Aguiar, A. Kalytta, A. Reller, A. Weidenkaff, S.G. Ebbinghaus, J. Mater. Chem. 18 (2008) 4260.
- [15] A. Kasahara, K. Nukumizu, T. Takata, J.N. Kondo, M. Hara, H. Kobayashi, K. Domen, J. Phys. Chem. B 107 (2003) 791.
- [16] L. Shuiping, T. Lianjiang, Z. Yu, C. Yanmo, J. Phys.: Conf. Ser. 188 (2009) 1.
- [17] T. Moriga, D. Aoki, Y. Nishida, K. Kitaji, K. Takahara, K. Murai, I. Nakabayashi, Phys. Status Solidi 203 (2006) 2818.
- [18] K. Sivula, F. Le Formal, M. Grätzel, ChemSusChem 4 (2011) 432.
- [19] W. Luo, Z. Li, X. Jiang, T. Yu, L. Liu, X. Chen, J. Ye, Z. Zou, Phys. Chem. Chem. Phys. 10 (2008) 6717.